Production of ϕ and ω Mesons in Near-Threshold pp Reactions

F. Balestra,[4] Y. Bedfer,[3] R. Bertini,[3,4] L. C. Bland,[2] A. Brenschede,[8,*] F. Brochard,[3] M. P. Bussa,[4] V. Chalyshev,[1] Seonho Choi,[2] M. Debowski,[6] M. Dzemidzic,[2] I. V. Falomkin,[1] J.-Cl. Faivre,[3] L. Fava,[4] L. Ferrero,[4] J. Foryciarz,[6,7] V. Frolov,[1] R. Garfagnini,[4] D. Gill,[10] A. Grasso,[4] E. Grosse,[5,†] S. Heinz,[3] V. V. Ivanov,[1] W. W. Jacobs,[2] W. Kühn,[8] A. Maggiora,[4] M. Maggiora,[4] A. Manara,[3,4] D. Panzieri,[4] H.-W. Pfaff,[8] G. Piragino,[4] G. B. Pontecorvo,[1] A. Popov,[1] J. Ritman,[8] P. Salabura,[6] P. Senger,[5] J. Stroth,[9] F. Tosello,[4] S. E. Vigdor,[2] and G. Zosi[4]

(DISTO Collaboration)

[1]*JINR, Dubna, Russia*
[2]*Indiana University Cyclotron Facility, Bloomington, Indiana*
[3]*Laboratoire National Saturne, CEA Saclay, France*
[4]*Dipartimento di Fisica "A. Avogadro" and INFN, Torino, Italy*
[5]*Gesellschaft für Schwerionenforschung, Darmstadt, Germany*
[6]*M. Smoluchowski Institute of Physics, Jagellonian University, Kraków, Poland*
[7]*H. Niewodniczanski Institute of Nuclear Physics, Kraków, Poland*
[8]*II. Physikalisches Institut, University of Gießen, Gießen, Germany*
[9]*Institut für Kernphysik, University of Frankfurt, Frankfurt, Germany*
[10]*TRIUMF, Vancouver, Canada*

(Received 26 August 1998)

The ratio of the exclusive production cross sections for ϕ and ω mesons has been measured in pp reactions at $T_{\text{beam}} = 2.85$ GeV. The observed ϕ/ω ratio is $(3.7 \pm 0.7^{+1.2}_{-0.9}) \times 10^{-3}$. After phase space corrections, this ratio is about a factor of 10 enhanced relative to naive predictions based upon the Okubo-Zweig-Iizuka rule, in comparison to an enhancement by a factor of $\sim$3 previously observed at higher energies. The modest increase of this enhancement near the production threshold is compared to the much larger increase of the ϕ/ω ratio observed in specific channels of $\bar{p}p$ annihilation experiments. [S0031-9007(98)07664-9]

PACS numbers: 25.40.Ve, 13.75.Cs, 13.85.Hd, 14.40.Cs

It is by now widely accepted that the nucleon's structure is substantially more complex than the simplest picture of three valence quarks. Pioneering results from deep-inelastic lepton scattering have revealed the importance of sea-quark and gluon contributions to the nucleon structure functions. In this context, the question has been raised as to what extent heavier quark pairs contribute to the nucleon wave function.

Experimental information on the nucleon's structure functions with polarized beams [1] and the $\Sigma_{\pi N}$ term in pion nucleon elastic scattering [2,3] suggest a significant contribution of strange sea quarks to the nucleon's wave function. In addition, $\bar{p}p$ annihilation studies [4] have observed that ϕ and ω meson cross section ratios are enhanced by up to 2 orders of magnitude relative to predictions based on a naive application of the Okubo-Zweig-Iizuka (OZI) rule [5]. According to the OZI rule, processes with disconnected quark lines in the initial or final state are suppressed. As a consequence of the near ideal mixing of the SU(3) singlet ω_1 and octet ω_8 states, the production of the ϕ meson should be strongly suppressed compared to the ω meson in reactions of hadrons with negligible strange quark content. In fact, the small deviation from the ideal mixing angle can be used to estimate the ϕ to ω cross section ratio to be $R/f \approx 4 \times 10^{-3}$ [6,7], where f is the ratio of the phase space factors (i.e., when assuming an energy independent matrix element).

It should be pointed out that the observed apparent violation of the OZI rule in $\bar{p}p$ is most dramatic for channels with the following features: (i) dominance of S-wave annihilations, (ii) low relative momentum of the $\bar{p}p$ system, and (iii) large invariant momentum transfer to the ϕ meson. These findings have been interpreted in terms of a polarized intrinsic $s\bar{s}$ contribution [7] to the nucleon's wave function, which would yield OZI-allowed quark-line diagrams for ϕ meson production. Alternatively, kaon exchange models involving two step processes [8,9] have been proposed to explain the ϕ meson production. Further insight into the origin of the enhanced ϕ/ω ratio in $\bar{p}p$ could be provided by studying near-threshold proton-proton reactions, where the kinematics are similar to $\bar{p}p$ but predictions based upon intrinsic strangeness in the nucleon and kaon exchange models might be expected to differ.

The existing proton-proton data above $\sqrt{s} = 4$ GeV show a slight enhancement with respect to predictions based on the OZI rule [10]. Unfortunately, there is a complete lack of data in the literature for ϕ meson production in pp reactions at energies close to the threshold. In this Letter, we report on the first measurement of the ϕ/ω cross section ratio at an available energy in the center

 0031-9007/98/81(21)/4572(4)$15.00

of mass of less than 100 MeV above the ϕ production threshold. In this experiment both meson channels were measured simultaneously.

The experimental setup (the DISTO spectrometer at SATURNE) is described in detail elsewhere [11]. A proton beam from the SATURNE proton synchrotron with kinetic energy $T_{\mathrm{beam}} = 2.85\,\mathrm{GeV}$ was directed onto a liquid hydrogen target of 2 cm length. Charged particles were tracked through a magnetic spectrometer and detected by a scintillator hodoscope and an array of water Čerenkov detectors. The magnetic spectrometer consisted of a dipole magnet (1.5 T), two sets of scintillating fiber hodoscopes inside the field, and two sets of multiwire proportional chambers (MWPC) outside the field. The large acceptance of the spectrometer ($\approx \pm 15°$ vertical, $\pm 48°$ horizontal) allowed for coincident detection of four charged particles, which was essential for the kinematically complete reconstruction of many final states ($pp\pi^+\pi^-$, $pp\pi^+\pi^-\pi^0$, ppK^+K^-, $pK\Lambda$, $pK\Sigma$). Particle identification and 4-momentum conservation served as powerful tools for background rejection. Event readout was triggered by a multiplicity condition on the scintillating fiber and hodoscope detectors, selecting events with at least three charged particles. In total, 1.3×10^7 events with four charged particles in the detector acceptance and a vertex inside the liquid hydrogen target were reconstructed.

Particle identification was achieved using the light output from the water Čerenkov detectors, which provided good π^+-proton separation spanning a wide range of momentum, as well as $K^\pm$ identification in a restricted range above the kaon Čerenkov threshold $p_{K,\mathrm{th}} = M_K c/\sqrt{n^2 - 1}$. Water was chosen as the Čerenkov radiator ($n = 1.33$, $p_{K,\mathrm{th}} = 560\,\mathrm{MeV}/c$) in order to match the momentum range of the kaons from the reaction $pp \to ppK^+K^-$, which is distributed around 700 MeV/c.

The reaction $pp \to pp\omega$ was identified via the $\pi^+\pi^-\pi^0$ decay of the ω meson (branching ratio 88.8%). Since the π^0 decays primarily into two photons (branching ratio 98.8%) and is therefore not detected in the spectrometer, this channel is identified via a missing mass analysis. For this analysis the 4-particle missing mass ($M_{\mathrm{miss}}^{pp\pi^+\pi^-}$) and the 2-particle missing mass (M_{miss}^{pp}) must correspond to a missing π^0 and a missing ω, respectively. The spectrum of $(M_{\mathrm{miss}}^{pp})^2$ is shown in Fig. 1 after selecting events of the type $pp\pi^+\pi^-$ based on the Čerenkov signals and requiring $0.0 < (M_{\mathrm{miss}}^{pp\pi^+\pi^-})^2 < 0.04\,\mathrm{GeV}^2/c^4$. This spectrum shows prominent signals from the $\pi^+\pi^-\pi^0$ decay of both the ω and η mesons.

The reaction $pp \to pp\phi$ was observed via the K^+K^- decay of the ϕ meson (branching ratio 49.1%), where the kaons are identified using the water Čerenkov detector. Since all four particles in the ppK^+K^- final state are detected, events of this type are kinematically overdetermined. Thus, an additional, drastic background

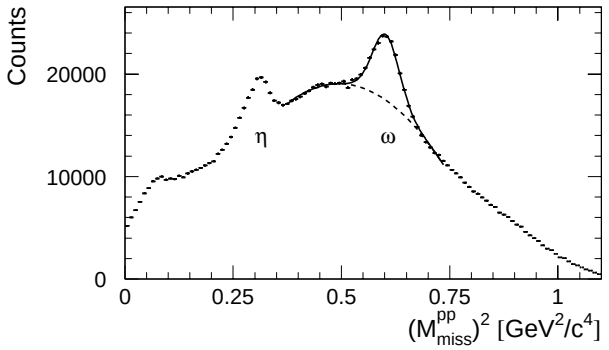

FIG. 1. Raw spectrum of $(M_{\mathrm{miss}}^{pp})^2$ for events of the type $pp\pi^+\pi^-\pi^0$ after selecting a missing π^0 via $M_{\mathrm{miss}}^{pp\pi^+\pi^-}$. This projection shows signals corresponding to the reactions $pp \to pp\omega \to pp\pi^+\pi^-\pi^0$ and $pp \to pp\eta \to pp\pi^+\pi^-\pi^0$. The structure near $(M_{\mathrm{miss}}^{pp})^2 \approx 0.1$ results from feedthrough of the $pp\pi^+\pi^-$ final state.

suppression can be achieved by requiring 4-momentum conservation. In this case, the invariant mass of the kaon candidates ($M_{\mathrm{inv}}^{K^+K^-}$) must equal M_{miss}^{pp}. This is demonstrated in Fig. 2, where the yield is plotted as a function of $(M_{\mathrm{inv}}^{K^+K^-})^2 - (M_{\mathrm{miss}}^{pp})^2$. The upper histogram shows the raw distribution, and the lower histogram corresponds to the remaining distribution after kaon conditions have been applied to the Čerenkov amplitude. The narrow peak near $(M_{\mathrm{inv}}^{K^+K^-})^2 - (M_{\mathrm{miss}}^{pp})^2 = 0.0$ results from events of the type ppK^+K^-. The peak near $0.9\,\mathrm{GeV}^2/c^4$ is from misidentified events of the type $pp\pi^+\pi^-$ which survived the Čerenkov conditions. After applying an additional requirement that $|(M_{\mathrm{inv}}^{K^+K^-})^2 - (M_{\mathrm{miss}}^{pp})^2| < 0.08\ \mathrm{GeV}^2/c^4$, a sample of ppK^+K^- events can be selected with a signal-to-background ratio of 4. The background is due primarily to incorrectly reconstructed events and forms a structureless contribution to the K^+K^- invariant mass distribution presented below.

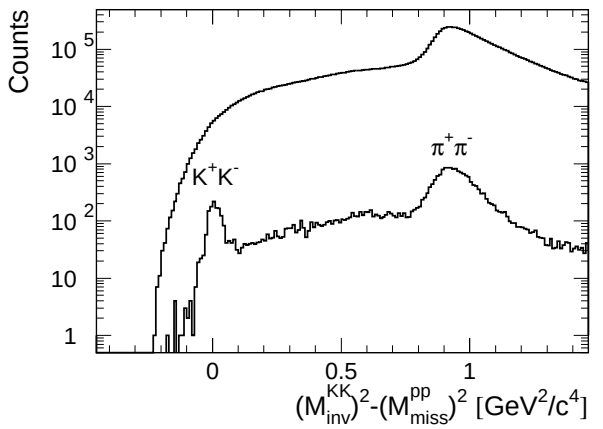

FIG. 2. Kinematical identification of ppK^+K^- events. Plotted here is the yield as a function of the difference $(M_{\mathrm{inv}}^{K^+K^-})^2 - (M_{\mathrm{miss}}^{pp})^2$, assuming that the mesons have the kaon mass. The upper histogram is the raw distribution, and the lower histogram is for a sample which is preselected by Čerenkov kaon conditions.

The raw distribution of $M_{\mathrm{inv}}^{K^+K^-}$ for events in the ppK^+K^- peak of Fig. 2 is shown in the top frame of Fig. 3. It can be seen that a large fraction of the K^+K^- pairs is produced via an intermediate ϕ meson. The mass range displayed corresponds to the kinematically allowed region, where the lower bound is given by the rest mass of the decay kaons, and the upper bound is defined by the available energy. The K^+K^- invariant mass spectrum shown in the lower frame has been corrected for the detector acceptance and analysis efficiency over the full mass range, as described below. This spectrum has been fit with the sum of a background contribution and a peak from the ϕ resonance. The shape of the background was assumed to be given by the $M_{\mathrm{inv}}^{K^+K^-}$ distribution for an ensemble of events that are uniformly distributed according to 4-body (ppK^+K^-) phase space. The shape of the ϕ resonance was given by the natural line shape folded with a Gauss function to account for the detector resolution. When treating the width of the Gaussian as a free parameter, a width of $\sigma = 3.7 \pm 0.5$ MeV/c^2 is determined in comparison to a resolution of 3.4 ± 0.1 MeV/c^2 obtained from simulations of the detector performance.

The relative acceptance of the apparatus for the $pp\omega$ and $pp\phi$ channels has been evaluated by means of Monte Carlo simulations, which, after digitization, were processed through the same analysis chain as the measured data. The acceptance could be determined independent of the actual phase space distribution of the particles in the final state, because the following two requirements are fulfilled with the DISTO spectrometer: (i) After accounting for the azimuthal and reflection symmetries, the detector acceptance was nonzero over the full kinematically allowed region; (ii) the detector acceptance was determined as a function of all relevant degrees of freedom in the final state. In order to determine the acceptance as a function of these degrees of freedom, the kinematically allowed phase space was divided into multidimensional bins of suitable coordinates and the efficiency was simulated for each bin separately. This procedure was carried out separately in five and four dimensions for the ϕ and ω meson production, respectively.

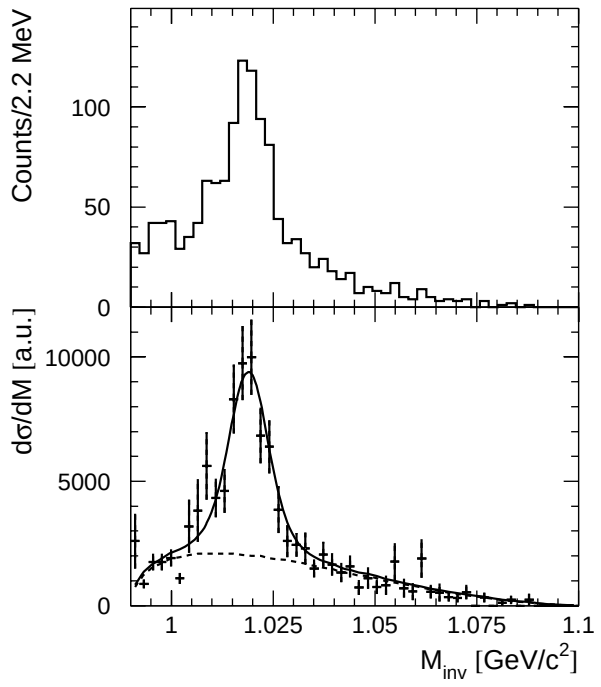

FIG. 3. Top frame: raw distribution of the K^+K^- invariant mass for ppK^+K^- events. The ϕ meson at 1.019 GeV/c^2 is clearly visible. Bottom frame: $M_{\mathrm{inv}}^{K^+K^-}$ distribution after efficiency corrections over the full mass range. The dashed curve represents the background contribution and the solid curve shows the sum of the background and the resonant contribution.

Although the reaction mechanism could produce spin alignment [12], the observed angular distributions of the ϕ and ω decays are consistent with the isotropic distribution assumed in the simulations. Furthermore, the matrix element of the $\omega \to \pi^+\pi^-\pi^0$ decay was taken from [13] and verified to be consistent with the data from [14,15].

After application of the full acceptance corrections and correcting for the decay branching ratios, the production ratio $pp \to pp\phi/pp \to pp\omega$ is determined to be $(3.7 \pm 0.7^{+1.2}_{-0.9}) \times 10^{-3}$, where the first error is statistical and the second error range is due to systematic uncertainty. The experimental uncertainties are dominated by systematic errors arising mainly from the simulation of the relative efficiencies for ω and ϕ detection and the determination of the efficiencies of the particle identification. However, since both meson channels have been detected in events with four charged particles and measured within the same experiment, many possible systematic uncertainties, such as those related to determining the absolute luminosity, cancel when considering the production ratio.

In Fig. 4, the ϕ/ω ratio (filled square) is compared to data at higher energies taken from the literature [10]. All error bars shown are the sum of systematic and statistical errors. The dashed line corresponds to the OZI prediction multiplied by the ratio of available 3-body phase space for ϕ to ω production. The solid line results from a recent model calculation by Sibirtsev [16]. In this model, ϕ and ω production arise from the known coupling to the πp channel, taking into account the pp final state interaction. Similar calculations by Titov *et al.* [17] predict a ϕ meson production rate consistent with that of Sibirtsev. Although the higher energy data agree well with the predictions of Sibirtsev, near threshold the measured ratio is enhanced by about a factor of 3.

The angular distributions of the ϕ and ω mesons are shown in Fig. 5. Since the entrance channel is symmetric, the observed symmetry about $\cos(\Theta_{\mathrm{cm}}) = 0$ is expected and increases confidence in the acceptance corrections. From the upper distribution we conclude that the ϕ meson is predominantly in a S-wave state relative to the pp system. The ω meson's angular distribution has been fit

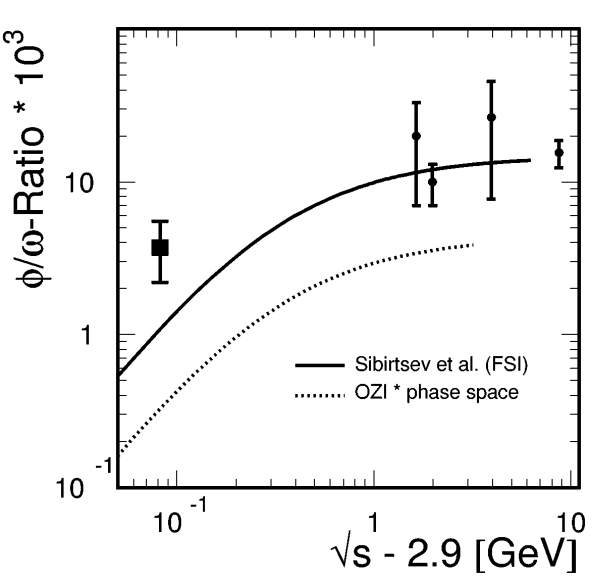

FIG. 4. Ratio of the exclusive total cross sections for the $pp\phi$ and $pp\omega$ reactions as a function of the available energy above the ϕ production threshold. Shown is the value measured in this work (square) together with data at higher energies and model calculations described in the text.

with an expansion using the first three even Legendre polynomials. The deviations from isotropy indicate that higher partial waves are involved in the ω production. These angular distributions may provide additional constraints for model calculations of vector meson production, such as those of Nakayama *et al.* [18].

In conclusion, the production of vector mesons has been studied in pp reactions at $T_{\text{beam}} = 2.85$ GeV. Clear signals of η, ω, and ϕ mesons have been observed by measuring their charged decay products. The ϕ/ω cross section ratio has been measured and is observed to exceed a naive application of the OZI rule by

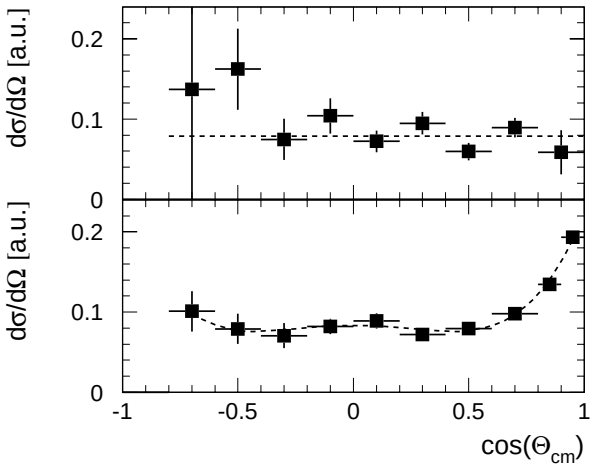

FIG. 5. Angular distribution of the ϕ and ω mesons (top and bottom, respectively). The error bars indicate only the statistical errors and the curves show a fit with the sum of even Legendre polynomials.

an order of magnitude. Although calculations using the known $\phi - \pi p$ coupling are able to explain the enhancement observed at higher energies, these predictions still underestimate the near-threshold behavior by a factor of 3. However, more refined calculations may well provide an explanation for this increase without explicitly requiring a significant contribution of $s\bar{s}$ to the nucleon's wave function. This observed increase of the ϕ/ω ratio near threshold is less dramatic than the rise of the ϕ/ω ratio in $\bar{p}p$ annihilation at low relative momenta. Thus, it would be very useful to study the evolution of the ϕ/ω ratio at energies even closer to the production threshold.

This work has been supported in part by the following agencies: CNRS-IN2P3, CEA-DSM, NSF, INFN, KBN (2 P03B 117 10 and 2 P03B 115 15), and GSI.

*Present address: Brokat Infosystems AG-Stuttgart, Germany.
†Present address: FZ-Rossendorf and TU Dresden, Germany.

[1] J. Ashman *et al.*, Phys. Lett. B **206**, 364 (1988); Nucl. Phys. **B328**, 1 (1989); P. Amandruz *et al.*, Phys. Lett. B **295**, 159 (1992).
[2] T. P. Cheng and R. F. Dashen, Phys. Rev. Lett. **26**, 594 (1971).
[3] T. P. Cheng, Phys. Rev. D **13**, 2161 (1976); J. Gasser *et al.*, Phys. Lett. B **213**, 85 (1988); J. Gasser, H. Leutwyler, and M. E. Sainio, Phys. Lett. B **253**, 252 (1991).
[4] J. Reifenrither *et al.*, Phys. Lett. B **267**, 299 (1991); V. G. Ableev *et al.*, Phys. Lett. B **334**, 237 (1994); C. Amsler *et al.*, Phys. Lett. B **346**, 363 (1995).
[5] G. Zweig, CERN Report No. 8419/Th 412, 1964; S. Okubo, Phys. Lett. **5B**, 165 (1965); I. Iizuka, Prog. Theor. Phys. Suppl. **37–38**, 21 (1966); S. Okubo, Phys. Rev. D **16**, 2336 (1977).
[6] H. J. Lipkin, Phys. Lett. **60B**, 371 (1976).
[7] J. Ellis, Phys. Lett. B **353**, 319 (1995).
[8] Ulf-G. Meißner *et al.*, Phys. Lett. B **408**, 381 (1997).
[9] M. P. Locher and Yang Lu, Z. Phys. A **351**, 83 (1994); D. Buzatu and F. M. Lev, Phys. Rev. C **51**, R2893 (1995); O. Gortchakov *et al.*, Z. Phys. A **353**, 447 (1996).
[10] V. Blobel *et al.*, Phys. Lett. **59B**, 88 (1975); R. Baldi *et al.*, Phys. Lett. **68B**, 381 (1977); M. W. Arenton *et al.*, Phys. Rev. D **25**, 2241 (1982); S. V. Golovkin *et al.*, Z. Phys. A **359**, 435 (1997).
[11] F. Balestra *et al.*, Nucl. Instrum. Methods (to be published); R. Bertini, Nucl. Phys. **A585**, 265c (1995); A. Maggiora, Nucl. Phys. News **5**, No. 4, 23 (1995).
[12] M. P. Rekalo, J. Arvieux, and E. Tomasi-Gustafsson, Z. Phys. A **357**, 133 (1997).
[13] P. Lichard, Phys. Rev. D **49**, 5812 (1994).
[14] M. Stevenson *et al.*, Phys. Rev. **125**, 687 (1962).
[15] P. Weidenaur *et al.*, Z. Phys. C **59**, 387 (1993).
[16] A. Sibirtsev, Nucl. Phys. **A604**, 455 (1996); (private communication).
[17] A. I. Titov, B. Kämpfer, and V. V. Shklyar, nucl-th/9712024.
[18] K. Nakayama *et al.*, Phys. Rev. C **57**, 1580 (1998).